Journal: Computers and Geotechnics

Year: 2013

Hydro-mechanical hypoplastic models for unsaturated soils under isotropic stress conditions

W. Fuentes *, Th. Triantafyllidis

Institute of Soil Mechanics and Rock Mechanics, Karlsruhe Institute of Technology KIT, Engler-Bunte-Ring 14, 76131 Karlsruhe, Germany

A B S T R A C T

The current work presents two hypoplastic models to predict the hydraulic and mechanical behavior of the unsaturated soils. The hydraulic model is capable to reproduce the observed hysteretic behavior for the drying and wetting processes and incorporates the void ratio dependence. The mechanical model is written in terms of the Bishop effective stress and is limited only to isotropic states. It incorporates a normal consolidation line that depends on the degree of saturation. Both models were developed under the hypoplastic framework and therefore are capable to simulate the observed behavior without defining a yield surface. Simulations of some experiments performed with Pearl clay suggest that the models accurately predict its hydro-mechanical behavior.

Keywords:
Unsaturated soils
Hypoplasticity
Coupled models
Retention curve
Modeling

1. Introduction

For many authors, the Theory of Porous Media TPM serves as theoretical background to deduce the equations that govern the hydro-mechanical behavior of the unsaturated soils [1–5]. Its solution requires the introduction of at least two constitutive models, one governing the mechanical behavior of the soil and the second describing the hydraulic behavior of the water in the pores [4]. The first interrelates incrementally a constitutive stress $\bar{\boldsymbol{\sigma}}$ [6] with the solid deformation $\boldsymbol{\varepsilon}$ whereas the second links the degree of saturation S_w with the suction $s = p_a - p_w$ defined as the difference between the pore air pressure p_a and the pore water pressure p_w.

It is well accepted that the agreement of the simulations with the observed experimental behavior is only possible by coupling the hydraulic and mechanical constitutive models [7–12]. Since the work of Alonso et al. [13], a large number of mechanical constitutive models incorporated the dependence of the hydraulic variables (s and S_w) and have performed well on the simulation of some experimental curves (see [14,6,15,11] for extensive review of models). A first generation of models were based on the net stress $\boldsymbol{\sigma}^{\text{net}}$ (as constitutive stress) which in terms of the total stress $\boldsymbol{\sigma}^{\text{tot}}$ is defined as $\boldsymbol{\sigma}^{\text{net}} = \boldsymbol{\sigma}^{\text{tot}} + p_a\mathbf{1}$ [16–18].[1] Nevertheless, they could not reproduce a smooth transition between saturated and unsaturated sates and could not describe a unique critical state in the stress space [6,10,11,14]. These facts and others motivated a second generation of models to choose the Bishop stress $\boldsymbol{\sigma} = \boldsymbol{\sigma}^{\text{tot}} + p_a\mathbf{1} - \chi s\mathbf{1}$ as constitutive stress instead, where χ is the Bishops parameter, e.g. [19–24,9] among others. Notice that most of the reported models in the literature and all the ones cited herein where developed under the elasto-plastic framework.

For all these elasto-plastic models, the introduction of a loading-collapse surface to reproduce the volume contraction upon wetting is evidently the most popular approach since its original formulation in [13] (see analysis of this approach in [25,11,14]). For isotropic states, this approach leads to a normal consolidation line NCL which depends on the current state (s,S_w) and can be defined in the semi-log space of the mean constitutive stress $\bar{p} = -1/3\ \text{tr}(\bar{\boldsymbol{\sigma}})$ and the void ratio e by introducing the reference void ratio N ($e = N$ for $\bar{p} = 1$ kPa) and the compression index λ. Under this scheme, the initialization of the preconsolidation pressure $p_c = p_{c0}$ and the adopted functions for N and λ turns out to be the crucial key that guarantees the success of the model [14]. Finding a method to determine the initial value p_{c0} is not an easy task. Just as an example, Sun et al. [26] related p_{c0} with the initial void ratio e_0 and the current suction s, but doing this allows one to interpret e_0 as an additional material parameter. Let us add the fact that many models are calibrated with dried slurry samples, and thereby the value of p_{c0} at the isotropic compression curve is hardly identifiable due to the stiffness smooth degradation. With respect to the functions N and λ, the model of Galipolli et al. [21] proposed a dependence with the suction s and degree of saturation S_w by incorporating the so-called bounding factor $\xi = \xi(s,S_w)$ representing the magnitude of the interparticle bonding due to water

menisci. Despite of its simplicity and good performance on the simulations, it was not absent from critics; Sheng [14] and Zhou et al. [27] pointed out that this model can produce a yield surface expansion at neutral loading when the suction rises $\dot{s} > 0$ while the mean Bishop stress remains constant p = const, which reveals the model weakness on the intend to fulfill some of the plasticity theory principles. This and other findings motivated Zhou et al. [27] to develop a novel compression law based on the Bishop stress $\boldsymbol{\sigma}$ whereby N is a constant and the compression index $\lambda = \lambda(S_w)$ depends only on the degree of saturation S_w. Surprisingly, with the new formulation the model is able to reproduce most of the capabilities from other models (e.g. as in [21]) and eliminates the limitations commented in [14]. However, the fact that N is a constant disables the model to simulate very loose materials exhibiting macropores where eventually the void ratio e could reach values above N, as for example unsaturated silty sand prepared with the moist-tamping method. Above this, let us add that the loading-collapse surface looses its convexity in the transition from saturated to unsaturated states [24,14], fact which demands sophisticated integration algorithms [24,28,29] in order to obtain reliable numerical results. At this point, we note that models which do not require the definition of a yield surface as in hypoplasticity, could be advantageous on their extension for unsaturated soils.

Unfortunately, most of the hypoplastic models for the mechanical behavior of soils are limited to saturated materials [30–33]. Just a few exceptions are found in the literature intended to model the unsaturated soils [34–37]. The model from Niemunis [36] was formulated with a modified Bishop stress proposed by Gudehus [34]. This effective stress is able to simulate volumetric contraction upon wetting observed at isotropic states. Nevertheless, the formulation of the constitutive model did not couple the hydraulic variables and therefore the observed shift of the normal consolidation line (or maximum void ratio line for the case of the hypoplastic version of [30]) is not reproduced. The model from Bauer et al. [35] actually limited its capabilities to monotonic tests under constant gravimetric water content w, fact which disables the possibility to simulate the coupled effects under wetting or drying loading. Probably the most successful model under this framework is the one proposed by Masin and Khalili [37] which is based on the Khalili and Khabbaz effective stress [38]. In contrast to its precedents, this model coupled the hydraulic variables in its formulation. The main limitation actually lies in the selected effective stress (and not on the model) which is not able to distinguish between drying-wetting cycles provided its dependence only with the suction (see [6,10,11] for a discussion). This can be corrected by adopting for example the effective stress proposed by the Khalili and Zargarbashi in [39].

Regarding to the hydraulic constitutive models, basically one can group them into two categories. The first category corresponds to injective functions relating the degree of saturation S_w and the suction s with the general form:

$$S_w = S_w(s) \tag{1}$$

implying a unique relation between s and S_w. Well known examples are Gardner [40], Brooks and Corey [41], van Genuchten [42], Fredlund and Xing [43] among others. All these models can be adjusted very good to a particular main branch, but due to its elastic nature they cannot reproduce the hysteretic behavior exhibited under cycles of wetting and drying.

Constitutive models belonging to the second category do not present this limitation because they are able to produce plasticity at the main branches. Outstanding examples from this category are the models from [8,9,22,23,26,44,45] among many others. All the cited models are formulated within the framework of one-dimensional elastoplasticity and present two yield surfaces, namely the main drying curve and the main wetting curve. These models are not wrong, and actually they reproduce very good the hysteretic behavior including in some cases the incorporation of the void ratio dependence. However, the literature shows an alternative framework which apparently promises similar capabilities without introducing elastoplastic concepts. An outstanding example is the model from Li [46] which employs in its formulation the last suction reversal point to simulate a smooth transition from a path starting in the "elastic" region and approaching to the main branches. This type of formulation, which later on we prove that follows a hypoplastic equation, showed that it is possible to reproduce most of the features exhibited by the elastoplastic models with a simple constitutive equation. Other approaches following a similar type of constitutive equation are found in [47,48], but they have self categorized as "bounding surface" models. The simplicity of these models probably motivated Zhou et al. [27] and Liu et al. [49] to examine the performance when coupling a "hypoplastic" hydraulic model with an elasto-plastic mechanical model. To the authors knowledge, two coupled hypoplastic models for the hydraulic and mechanical component have never been studied which motivates the development of the current work.

This article presents the development of two hypoplastic models for unsaturated materials, one describing the hydraulic component and the other describing the mechanical response. The hydraulic model capabilities include the simulation of the hysteretic behavior at drying and wetting cycles, and incorporates the dependence with the void ratio e. The mechanical model is able to reproduce the influence of the normal consolidation line with the degree of saturation S_w. We have organized the work with the following structure. At the beginning (Section 2) the equations of the hydraulic model without incorporating the void ratio effect are deduced. The extension for deformable materials is shown in Section 3 completing the formulation of the hypoplastic model for the hydraulic component. For the mechanical response, a hypoplastic model is also proposed in Section 4. A short guide to understand and calculate the material parameters is given in Section 6 and some simulations to evaluate the model predictive capabilities are given in Section 7.

2. Hydraulic model for non-deformable materials

In this section we develop a rate-type constitutive model for the hydraulic component linking only the degree of saturation S_w with the suction s. The proposed model adopts a particular equation to describe the main branches similar to others [46,48,27,49]. Let us represent the equation for the main drying curve as $S_w = S_w^d(s)$ and for the main wetting curve as $S_w = S_w^i(s)$[2] as depicted in Fig. 1a. The symbols s^d and s^i represent the projection of Point A (see Fig. 1a) at the main branches under constant degree of saturation S_w. Hence, one can establish the following general relation:

$$s^d = s^d(S_w) \quad s^i = s^i(S_w) \tag{2}$$

Let us term the "bounding branch" denoted by $S_w = S_w^{d/i}(s)$ as the main branch that serves as bounding surface for the current state and the suction rate direction $\dot{s}$. More specifically, for a process of drying $\dot{s} > 0$, the bounding branch corresponds to the main drying curve $S_w^{d/i} = S_w^d(s)$ whereas for a process of wetting $\dot{s} < 0$ corresponds to the main wetting curve $S_w^{d/i} = S_w^i(s)$. If the current state (s,S_w) lies at its bounding branch, a suitable constitutive model is:

$$\dot{S}_w = \frac{\partial S_w^{d/i}}{\partial s}\dot{s} \quad \text{for} \quad S_w = S_w^{d/i}(s) \tag{3}$$

Nevertheless, for other states different than this ($S_w \neq S_w^{d/i}(s)$) the hydraulic behavior does not follow Eq. (3) and therefore a modification must be introduced. The experiments show that the slope $\partial S_w/\partial s$ is smaller for states between the main branches $S_w \neq S_w^{d/i}(s)$.

[2] The superindex "i" stands from inbibition.

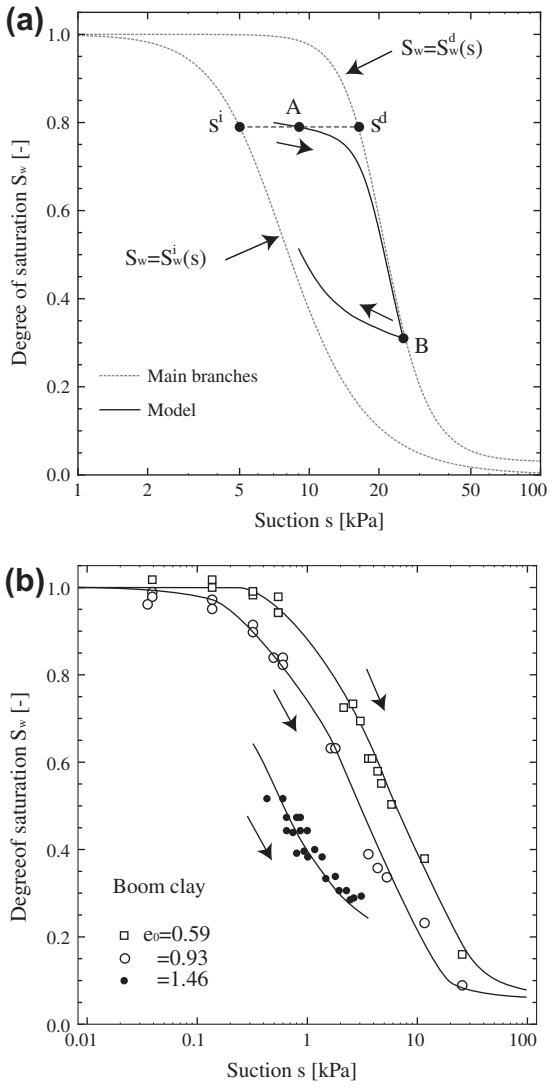

Fig. 1. (a) Projection of the suction in the main branches. (b) Influence of initial void ratio e_0 in the water retention curves. Data from [50].

Actually, the slope $\partial S_w/\partial s$ takes its minimum value after a reversal at the bounding branch, see for example Point B in Fig. 1a. In this case, the current slope $\partial S_w/\partial s$ can be calculated as:

$$\frac{\partial S_w}{\partial s} = \kappa_w \frac{\partial S_w^{d/i}}{\partial s}\dot{s} \quad \text{(minimum slope for current } S_w) \tag{4}$$

where $\kappa_w < 1$ is a material parameter. Let us propose the following constitutive model as an interpolation of the slopes given in Eqs. (3) and (4):

$$\dot{S}_w = \frac{\partial S_w^{d/i}}{\partial s}(\kappa_w - (1-\kappa_w)Y^{d/i})\dot{s} \tag{5}$$

where $Y^{d/i}$ $(0 \leqslant Y^{d/i} \leqslant 1)$ is an interpolation function and takes the function $Y^{d/i} = Y^d$ for a process of drying $(\dot{s} > 0)$ and $Y^{d/i} = Y^i$ for wetting $(\dot{s} < 0)$. In Appendix B it is shown that Eq. (5) has the same structure as a classical hypoplastic equation with the form $\dot{S}_w = L_s\dot{s} + N_s|\dot{s}|$. Some interpolation functions $Y^{d/i}$ have been already proposed in the literature. For example, the model from Li [46] uses a logarithmic scale to perform the interpolation and introduces reversal points in its formulation. We do not consider reversal points because it might lead to overshooting when performing cycles with different suction amplitudes. On the other hand, the model from Zhou et al. [27] proposed a potential relation as the interpolation function, which might be advantageous because it needs only an additional parameter (the exponent). Nevertheless, the potential relation can overestimate the slope at wetting paths $(\dot{s} < 0)$ as seen in some simulations. By trial and error, we have experienced that by interpolating in a logarithmic scale of the suction, the predictive capabilities are improved. The proposed function is similar to the one proposed by [46] but without introducing reversal points:

$$\begin{aligned} Y^{d/i} = Y^d &= \left[\frac{\log(s/s^i)}{\log(s^d/s^i)}\right]^{n_w}, \quad \text{for } \dot{s} \geqslant 0 \\ = Y^i &= \left[\frac{\log(s^d/s)}{\log(s^d/s^i)}\right]^{n_w}, \quad \text{for } \dot{s} < 0 \end{aligned} \tag{6}$$

where the exponent $n_w \approx 1$–10 is a material parameter that controls the interpolation. To complete the model, we need to introduce the equations describing the main branches $S_w = S_w^d(s)$ and $S_w = S_w^i(s)$. Let us select the empirical models proposed by Brooks and Corey B& C [41] and van Genuchten vG [42] as examples. We rewrite their original models replacing the degree of saturation S_w with the effective degree of saturation S_e to simulate the residual water after a long drying process. The effective degree of saturation S_e depends on the residual degree of saturation denoted by S_{w0}. For the sake of generality, we assume that the drying and wetting processes may present different values of S_{w0}. Therefore it will be distinguished between the effective degree of saturation for the main drying curve S_e^d and main wetting curve S_e^i:

$$S_e^d = \frac{S_w - S_{w0}^d}{1 - S_{w0}^d}; \quad S_e^i = \frac{S_w - S_{w0}^i}{1 - S_{w0}^i} \tag{7}$$

where S_{w0}^d and S_{w0}^i are the residual degree of saturation for the main drying and wetting curve respectively and are model parameters.

Let us start with the model from Brooks and Corey B& C. For this case, the main branches are defined with the following functions:

$$S_e^d = \begin{cases} (a^d/s)^{\lambda^d}, & s > a^d \\ 1, & s \leqslant a^d \end{cases}; \quad S_e^i = \begin{cases} (a^i/s)^{\lambda^i}, & s > a^i \\ 1, & s \leqslant a^i \end{cases} \tag{8}$$

where λ^d, λ^i, a^d and a^i are the material parameters, the last two (a^d and a^i) representing the air entry suction in each of the main branches [41]. Notice that each curve needs three parameters (including the residual degree of saturation) and therefore a single rule to avoid the overlapping (when the wetting and drying curve cross each other) does not exist. But for example, by setting $S_{w0}^d = S_{w0}^i$, the curves do not overlap only if $\lambda^d \leqslant \lambda^i$.

For the van Genuchten model vG, the following relations are used:

$$S_e^d = \frac{1}{[1 + (\alpha^d s)^{n^d}]^{1-1/n^d}}; \quad S_e^i = \frac{1}{[1 + (\alpha^i s)^{n^i}]^{1-1/n^i}} \tag{9}$$

where α^d, α^i, n^d and n^i are the model parameters. Similar to the model of B& C, by setting $S_{w0}^d = S_{w0}^i$ and $\alpha^d < \alpha^i$, the curves do not overlap only if $n^d \leqslant n^i$.

The stiffness $\partial S_w^{d/i}/\partial s$ can be rewritten with the effective degree of saturation:

$$\frac{\partial S_w^{d/i}}{\partial s} = \frac{\partial S_e^{d/i}}{\partial s}\left(1 - S_{w0}^{d/i}\right) \tag{10}$$

Differentiation of Eq. (8) or (9) and replacing $s = s^{d/i}(S_w)$ yields to:

$$\frac{\partial S_e^{d/i}}{\partial s}(S_w) = \frac{\lambda^{d/i}(a^{d/i})^{\lambda^{d/i}}}{(s^{d/i})^{(\lambda^{d/i}+1)}} \quad \text{for B\&C;} \tag{11}$$

$$\frac{\partial S_e^{d/i}}{\partial s}(S_w) = (s^{d/i})^{(n^{d/i}-1)}(\alpha^{d/i})^{n^{d/i}} \times (1 + (s^{d/i}\alpha^{d/i})^{n^{d/i}})^{-2+1/n^{d/i}}(1 - n^{d/i}) \quad \text{for vG} \tag{12}$$

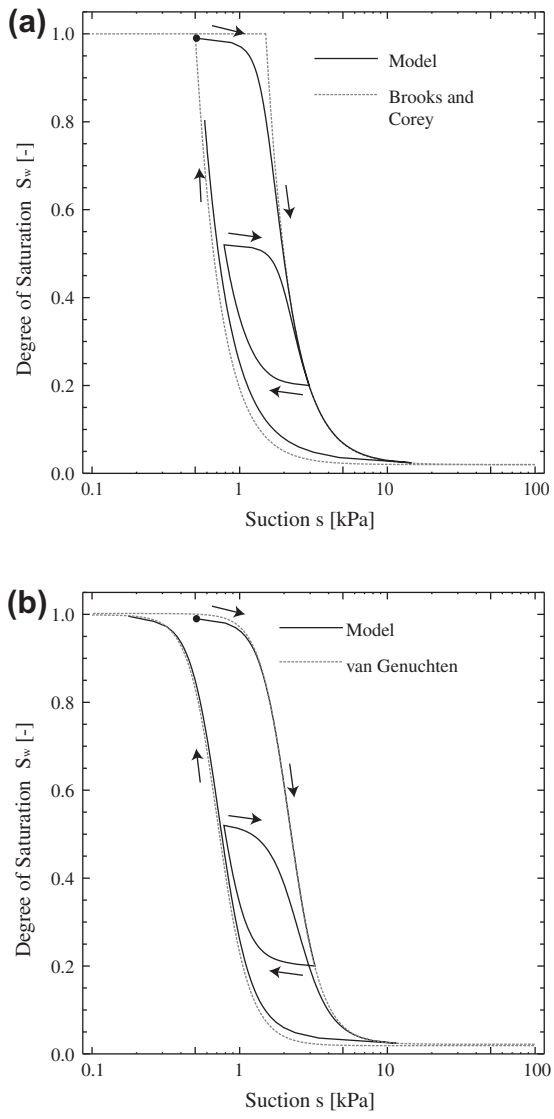

Fig. 2. Model simulation using for the main branches description the equation from (a) Brooks and Corey and (b) van Genuchten.

The projected suction $s^{d/i}(S_w)$ at the bounding branch $S_w^{d/i}$ is found by solving the suction s for the current degree of saturation S_w in Eq. (8) or (9) and setting $s = s^{d/i}(S_w)$. Fig. 2a and b shows some simulations using the Brooks and Corey and van Genuchten curves as main branches respectively

3. Extension of hydraulic model for deformable materials

In the last decades, the void ratio dependence in the main branches has been confirmed by several authors [50–54]. Fig. 1b shows the experimental results by Romero [50] using compacted Boom clay specimens with different initial densities which testify this dependence on the main drying curve. Other experiments also confirm that a similar effect is obtained for the main wetting curves [26].

Concerning to the constitutive modeling, the shift of the soil water characteristic curve SWCC can be obtained by different methods. The models from Sun et al. [26], Nuth et al. [54], Morvan et al. [44] and Masin [55] proposed a dependence between the air entry suction a and the void ratio e. The model from Galipolli et al. [52] established the equations of the main branches in the space $S_w - s - e$, which for constant void ratio $e = \text{const}$ is called "intrinsic water retention curve" IWRC after [54]. The model from Sheng et al. [45] found a first order differential equation which links the degree of saturation S_w and the initial void ratio e_0 for the main branches. The model from Wheeler [9] used the modified suction $s^* = ns$, where $n = e/(1+e)$ is the soil porosity, as primary variable to be consistent with the work-conjugated variables according to Houlsby [7] and succeed to reproduce the observed dependence with the void ratio e.

Probably the simplest approach corresponds to the concept of "intrinsic water retention curves" IWRC and we adopt it for our model. This approach proposes the following general form to describe the main branches:

$$S_w = S_w^d(s,e); \quad S_w = S_w^i(s,e) \tag{13}$$

A notable example was given by Gallipoli et al. [52] where the van Genuchten curve [42] was extended to incorporate the void ratio dependence (see Fig. 3 for an example). The extended van-Genuchten curves for the main drying curve $S_w = S_e^d(s,e)$ and main wetting curve $S_w = S_e^i(s,e)$ are accordingly described with the following functions:

$$S_e^d = \frac{1}{[1+(\alpha^d e^{m_e} s)^{n^d}]^{1-1/n^d}}; \quad S_e^i = \frac{1}{\left[1+(\alpha^i e^{m_e} s)^{n^i}\right]^{1-1/n^i}} \tag{14}$$

where $m_e \geqslant 0$ is a new material parameter and for $m_e = 0$ the original equation is recovered.

Differentiation of Eq. (14) together with Eq. (7) gives:

$$\begin{aligned}\dot{S}_w^{d/i} &= \frac{\partial S_w^{d/i}}{\partial s}\dot{s} + \frac{\partial S_w^{d/i}}{\partial e}\dot{e} \\ &= \left(1 - S_{w0}^{d/i}\right)\frac{\partial S_e^{d/i}}{\partial s}\dot{s} - (1 - S_{w0}^{d/i})\frac{\partial S_e^{d/i}}{\partial e}(1+e)\dot{\varepsilon}_v\end{aligned} \tag{15}$$

wherein $\dot{\varepsilon}_v = -\mathrm{tr}\dot{\boldsymbol{\varepsilon}}$ is the rate of volumetric deformation. The partial derivatives $\partial S_e^{d/i}/\partial s$ and $\partial S_e^{d/i}/\partial e$ are evaluated at the main branches and therefore they are deduced by differentiation of Eq. (13) and replacing with $s = s^{d/i}$:

$$\begin{aligned}\frac{\partial S_e^{d/i}}{\partial s}(S_w,e) = (s^{d/i})^{n^{d/i}-1}(\alpha^{d/i}e^{m_e})^{n^{d/i}} \times (1+(s^{d/i}\alpha^{d/i}e^{m_e})^{n^{d/i}})^{-2+1/n^{d/i}} \\ \times (1-n^{d/i});\end{aligned} \tag{16}$$

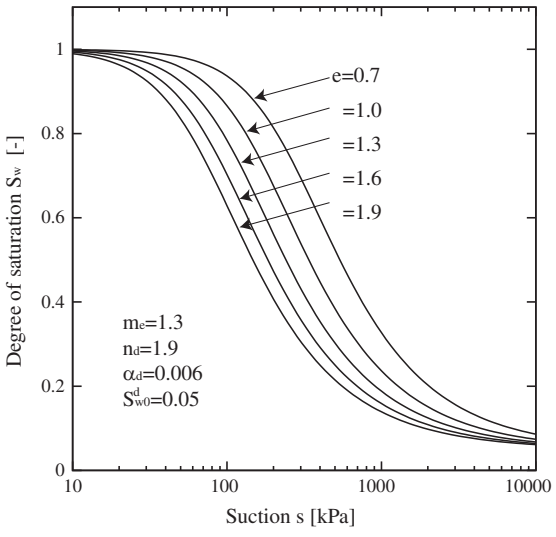

Fig. 3. Extended van Genuchten curve for deformable materials proposed by [52]. Intrinsic water retention curves IWRC for different void ratios e according to Eq. (19).

$$\frac{\partial S_e^{d/i}}{\partial e}(S_w, e) = -m_e(s^{d/i}e^{m_e}\alpha^{d/i})^{n^{d/i}} \times (1 + (s^{d/i}e^{m_e}\alpha^{d/i})^{n^{d/i}})^{1/n^{d/i}-2} \times (n^{d/i} - 1)/e \quad (17)$$

The new constitutive equation extended for deformable material is similar to Eq. (5) but with the additional term describing the void ratio dependence:

$$\dot{S}_w = (\kappa_w - (1 - \kappa_w)Y^{d/i})\frac{\partial S_w^{d/i}}{\partial s}\dot{s} - \frac{\partial S_w^{d/i}}{\partial e}(1 + e)\dot{\varepsilon}_v \quad (18)$$

We note in Eq. (18) that $\partial S_w^{d/i}/\partial e = \partial \dot{S}_w/\partial \dot{e}$. According to Sheng et al. [45], the derivative $\partial \dot{S}_w/\partial \dot{e}$ must fulfill two constraints; the first is that for full saturation $S_w = 1$ it vanishes $\partial \dot{S}_w/\partial \dot{e} = 0$. This can be easily proved by inspection of Eq. (17), which shows that $\partial \dot{S}_w/\partial \dot{e}$ is proportional to $(s^{d/i})^{n^{d/i}}$, factor which vanishes at $S_w = 1$ as well. The second constraint was postulated after experimental observation and establishes that under undrained conditions (constant gravimetric water content) and isotropic states, specimens subjected to wetting $\dot{s} < 0$ experience always volumetric contraction $\dot{e} < 0$ [45]. Accordingly, this is only possible if $\partial \dot{S}_w/\partial \dot{e} \geqslant -S_w/e$.

However, the deduction of the mentioned constraint did not consider the existence of a residual degree of saturation S_{w0}. In Appendix A we prove that the following constraint holds for undrained materials with $S_{w0} > 0$:

$$\frac{\partial \dot{S}_w}{\partial \dot{e}} \geqslant -\frac{S_w - S_{w0}}{e} \text{ for } \dot{s} < 0 \quad (19)$$

The above constraint can be examined in our proposed model for a wetting path lying at the main wetting curve. One can show that the model satisfies this constraint when:

$$m_e \leqslant (n^i - 1)^{-1} \quad (20)$$

which coincides with the result that one would obtain if applying the constraint given by [14] and supposing that there does not exist residual water $S_{w0} = 0$

4. Mechanical model for isotropic states

The mechanical model will be limited to the simulation of isotropic states and is developed within the framework of hypoplasticity [56,36]. The mean Bishop stress $p = (-1/3)\ \mathrm{tr}\ (\boldsymbol{\sigma})$ using $\chi = S_w$ is selected as constitutive stress and we set the air pressure $p_a = 0$ as reference. The selection of $\chi = S_w$ obeys to thermodynamical considerations which can be found in [7,5]. Considering the aforestated lines, we simplify the mean Bishop stress p to:

$$p = p^{\mathrm{net}} + S_w s \quad (21)$$

and by differentiation yields to:

$$\dot{p} = \dot{p}^{\mathrm{net}} + \dot{S}_w s + S_w \dot{s} \quad (22)$$

Let us briefly describe the hypoplastic model for the case of saturated states $S_w = 1$. The constitutive model is written in terms of the rate of the mean Bishop stress $\dot{p}$ (see Eq. (22)) and the rate of volumetric strain $\dot{\varepsilon}_v = -\mathrm{tr}(\dot{\boldsymbol{\epsilon}})$. [3] The general form of the constitutive equation is:

$$\dot{p} = K(\dot{\varepsilon}_v - Y_i|\dot{\varepsilon}_v|) \text{ for } S_w = 1 \quad (23)$$

where K is the Bulk modulus and Y_i is the degree of non-linearity for isotropic states. Due to the mathematical structure of Eq. (23), one can adjust the factors K and Y_i such that Eq. (23) coincides with a particular equation for isotropic loading $(\dot{\varepsilon}_v > 0)$ and unloading $(\dot{\varepsilon}_v < 0)$[4]. For this purpose, we introduce the maximum void ratio e_i as a function of the mean Bishop stress $e = e_i(p)$, which is equivalent with the normal consolidation line in the case of clays:

$$e = e_i(p) = e_{\mathrm{ref}} - \lambda \log\left(\frac{p}{p_{\mathrm{ref}}}\right) \quad (24)$$

where λ, e_{ref} and p_{ref} are material parameters. The Bulk modulus K is adjusted to reproduce the stiffness at the normal consolidation line and yields to the following relation:

$$K = \frac{(1 + e)p}{\lambda(1 - Y_{im})} \quad (25)$$

where Y_{im} corresponds to the maximum value of Y_i and is defined as:

$$Y_{im} = \frac{r_{Km} - 1}{r_{Km} + 1} \text{ with } r_{Km} = \lambda/\kappa \quad (26)$$

and r_{Km} represents the maximum value that can take the ratio between the bulk modulus for unloading and loading. The experiments indicate that these values are reached when the mean Bishop stress p lies at the maximum (Hvorslev) stress p_i for the current void ratio e which can be solved from Eq. (24):

$$p_i = p_{\mathrm{ref}} \exp\left(\frac{e_{\mathrm{ref}} - e}{\lambda}\right) \quad (27)$$

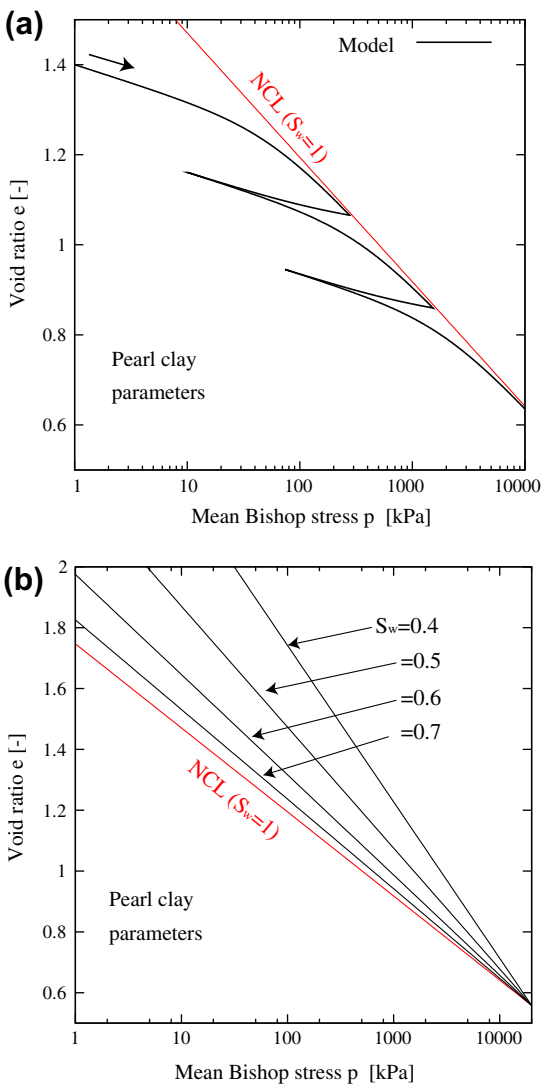

Fig. 4. (a) Simulation of isotropic test at saturated states $S_w = 1$. (b) Normal consolidation lines for different values of S_w.

[3] For $\dot{\varepsilon}_v$ and $\dot{p}$ compression is positive.

[4] see Appendix B for example with hydraulic model

Table 1
Material constants for hydraulic and mechanical model. The hydraulic model employs the extended van Genuchten equation for the main branches.

Symbol	Description	Units	Approx. range	Pear clay
Hydraulic model				
S_{w0}^d, S_{w0}^i	Residual degree of saturation	–	0–0.3	0.05, 0
α^d, α^i	Controls the air entry suction	–	0–2	6.5×10^{-4}, 0.05
n^d, n^i	Controls slope in SWCC	–	0.5–5	1.9, 1.5
m_e	Controls the void ratio dependence	–	0.0–5[a]	1.35
κ_w	Controls maximum stiffness of scanning curve	–	0.01–0.5	0.05
n_w	Controls transition of the slope in scanning curve	–	1–10	3
Mechanical model				
κ	Controls maximum stiffness at isotropic unloading	–	10^{-4}–0.1	0.02
λ^{sat}	Compression index of saturated NCL	–	10^{-3}–1	0.12
e_{ref}	Reference void ratio	–	0–2	0.5584
p_{ref}	Reference mean pressure	MPa	1–10^3	20
r_m	Controls λ for $S_w = 0$	–	1–10	6.7
n_S	Controls dependence of λ with S_w	–	1–5	3.7
n_u	Controls volume changes under wetting at $p < p_i$	–	1–10	2

[a] For m_e check Eq. (20).

In order to make a smooth transition between the overconsoldated and normally consolidated state, the factor Y_i is proposed to interpolate between the values $Y_i = 0$ at $p = 0$ and $Y = Y_{im}$ at $p = p_i$ as follows:

$$Y_i = \frac{r_K - 1}{r_K + 1} \tag{28}$$

$$r_K = 1 + (r_{Km} - 1)\left(\frac{p}{p_i}\right)^{n_r} \tag{29}$$

The exponent n_r controls the interpolation from Eq. (29) and is set in the current work to $n_r = 2$ for default. An example of isotropic test for saturated states is given in Fig. 4a using Pearl clay parameters (see Table 1), with two cycles of unloading–reloading. As all hypoplastic models, the proposed model presents always plastic accumulation and the normal consolidation line behaves as an asymptote for loading paths.

For unsaturated states, it is well accepted that the normal consolidation line depends additionally on the hydraulic variables s or S_w (or both). For constant suction $s = \text{const}$, some authors have shown that the position of the normal consolidation line is not fixed and it depends rather on the degree of saturation S_w [27]. Therefore we set the degree of saturation S_w as the only hydraulic variable describing the normal consolidation line, i.e. $e = e_i(p, S_w)$. We desire that the proposed model is capable of simulating very loose samples which can present very high void ratio e located above the normal consolidation line for $S_w = 1$. This would be consistent with proposal by Zhang et al. [57] who based on experimental results, proposed to translate the normal consolidation line in the vertical direction depending only on the degree of saturation S_w, or also with the model from Galipolli et al. [21] who presented an increasing reference void ratio N (for $p = 1$ kPa) and compression index λ with increasing bounding factor $\xi = \xi(s, S_w)$. On the other hand, the model from Zhou et al. [27] can simulate this particular state only if p is large enough considering that the reference void ratio $e = N$ is a constant, requirement imposed after observing that the model from Gallipoli et al. [21] fail the neutral loading test for constant Bishop mean stress $p = \text{const}$ and increasing suction $\dot{s} > 0$ (see Sheng [14]). We remind that the proposed model is hypoplastic, and therefore the normal consolidation line acts as an asymptote curve also known as "state boundary surface" [58] and not as a yield surface, i.e. its formulation is not subjected to any plasticity constraint.

For instance let us propose a normal consolidation line with increasing λ for decreasing S_w, such that the current state can reach high void ratios e for very low p. Fig. 4b illustrates the desired relation for several S_w, and shows that all of these lines intercept at the point with coordinates e_{ref} and p_{ref}, considered herein as material parameters. One might criticize this relation by pointing that for $p > p_{ref}$ the normal consolidation lines show an undesired response with the degree of saturation S_w, but we assume that the parameter p_{ref} is large enough (>5 MPa) to limit our model for stresses below this value or equivalently, that the samples can only reach such very high pressures only at saturated states $S_w = 1$. On the other hand one can propose other relations to avoid this shortcoming, e.g. and exponential relation in the e vs. p space, as in [59], but it would increase the complexity of the model. Hence, let us adopt the model schematized in Fig. 4b and propose the following equation for the compression index λ:

$$\lambda = \lambda^{sat} r \tag{30}$$

where $r = r(S_w)$ is a function of the degree of saturation S_w defined as:

$$r = 1 + (r_m - 1)(1 - S_w)^{n_S} \tag{31}$$

where r_m and n_S are material parameters. The parameter $r_m \geqslant 1$ is the value of r when $S_w = 0$, and n_S controls the interpolation between the states $S_w = 0$ and $S_w = 1$.

We note that the effect obtained for the normal consolidation line depicted in Fig. 4b is similar to the one proposed by Sun et al. [26], but therein they formulated the compression index λ as a function of the initial void ratio e_0 and the suction s.

So far the proposed equations simulate well the mechanical behavior as long as the degree of saturation S_w remains constant $\dot{S}_w = 0$. However, for changes of S_w or s the model is not able to reproduce the volumetric contraction ($\dot{\varepsilon}_v > 0$) observed sometimes during wetting. This effect can be modeled if we introduce the following term in the constitutive equation (Eq. (23)):

$$\dot{p} = K\left(\dot{\varepsilon}_v - Y_i|\dot{\varepsilon}_v| + y\langle -\dot{s}\rangle\sqrt{3}\right) \tag{32}$$

where $\langle -\dot{s}\rangle = -\dot{s}$ for $\dot{s} < 0$ and zero otherwise. We desire that $y = 0$ when $S_w = 1$ to be consistent with the model for full saturated case, constraint that will be proved later on. For normally consolidated states such that $e = e_i(p, S_w)$, the experiments show that during wetting $\dot{s} < 0$ under constant net stress $p^{net} = \text{const}$, the void ratio e remains always at the normal consolidation line described by the function $e = e_i(p, S_w)$ (see Eqs. (24), (30)). However, our model is based on the mean Bishop stress p and therefore it is simpler to calculate the amount of volumetric contraction that would be experienced under constant p rather than constant p^{net}. In the following lines, we will find an expression for y (see Eq. (32)) that reproduces this effect under $p = \text{const}$ and later on we will show that under

p^{net} = const a similar effect as in the experiments is obtained. This procedure presents a similar reasoning as the one presented in the work of Masin and Khalili [37], with the difference that we are considering a coupled hydraulic model.

For the case than $e = e_i(p, S_w)$, the volumetric strain rate $\dot{\varepsilon}_v$ at constant mean Bishop stress p = const is given by:

$$\dot{\varepsilon}_v = -\frac{1}{(1+e)}\frac{\partial e_i}{\partial S_w}\dot{S}_w \tag{33}$$

Replacing Eq. (33) in the relation $\dot{S}_w = (\partial \dot{S}_w/\partial \dot{\varepsilon}_v)\dot{\varepsilon}_v + (\partial \dot{S}_w/\partial \dot{s})\dot{s}$ results in:

$$\dot{S_w} = A\dot{s}$$
$$A = \frac{\partial \dot{S}_w}{\partial \dot{s}} \Big/ \left(1 + \frac{1}{(1+e)}\frac{\partial \dot{S}_w}{\partial \dot{\varepsilon}_v}\frac{\partial e_i}{\partial S_w}\right) \tag{34}$$

where A is a factor which gives $A = \partial \dot{S}_w/\partial \dot{s}$ for non-coupled hydraulic models and $A \neq \partial \dot{S}_w/\partial \dot{s}$ otherwise. If we replace Eqs. (33) and (34) in (32) and by imposing the constraints $\dot{p} = 0$ and $\dot{\varepsilon}_v > 0$ one obtains the following relation solved for y:

$$y = \frac{A}{\sqrt{3}}\frac{(Y_i - 1)}{(1+e)}\frac{\partial e_i}{\partial S_w} \quad (\text{for } e = e_i) \tag{35}$$

Notice that when $S_w = 0$ our hydraulic model gives $\partial \dot{S}_w/\partial \dot{s} = 0$ which results with $y = 0$. Hence at saturated states with $S_w = 1$ the model recovers the Eq. (23). The function y was derived for normally consolidated states whereby $p = p_i$. However, for overconsolidated states $p < p_i$ the experiments show that the volumetric contraction is much smaller (sometimes even expansion) and following [37], we multiply the function y by a factor f_u such that:

$$y = \frac{f_u A}{\sqrt{3}}\frac{(Y_i - 1)}{(1+e)}\frac{\partial e_i}{\partial S_w} \tag{36}$$

This factor is equal to one $f_u = 1$ when $p = p_i$ in order to recover the relation at Eq. (35) and less than one for overconsolidated states $p < p_i$:

$$f_u = \left(\frac{p}{p_i}\right)^{n_u} \tag{37}$$

By trial and error, we have found that setting $n_u \approx 2$ reproduces well the collapse behavior due to wetting at constant net stress of samples with different void ratios. Of course, the user may adjust n_u to improve the simulations. The derivative needed in Eq. (35) is:

$$\frac{\partial e_i}{\partial S_w} = n_s(r-1)(1-S_w)^{n_s-1}\lambda^{sat}\log(p/p_n) \tag{38}$$

Fig. 5 shows some simulations of volumetric contraction under wetting. If one starts at the point "a" located at the normal consolidation line for $S_w = 0.5$, and we apply a wetting path at constant mean Bishop stress p = const, the void ratio e decays till the NCL for $S_w = 1$ is reached. Note that the same effect happens when one starts at point "b" (also at the NCL for $S_w = 0.5$), but not when the initial point is below the NCL for $S_w = 1$, e.g. points "c" and "d". For those cases, the volumetric contraction is much smaller due that the factor f_u is less than one $f_u < 1$ (Eq. (37)). Taking into account that factor y was adjusted to constant Bishop stress p = const and not to constant net stress p^{net} = const, we proceed to examine the same wetting paths under p^{net} = const (dashed lines in Fig. 5). Paths starting at points "a" and "b" show a contractant behavior ending approximately below the NCL for $S_w = 1$. The path starting at point "d" show little contraction and the path starting at point "c" shows expansion, behavior which can be expected in overconsolidated samples.

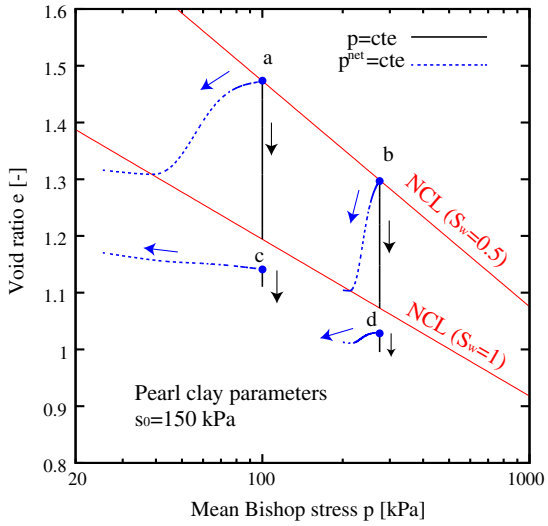

Fig. 5. Wetting paths at constant mean Bishop stress p = const and constant net stress p^{net} = const beginning with $S_w = 0.5$ and ending with $S_w = 1$.

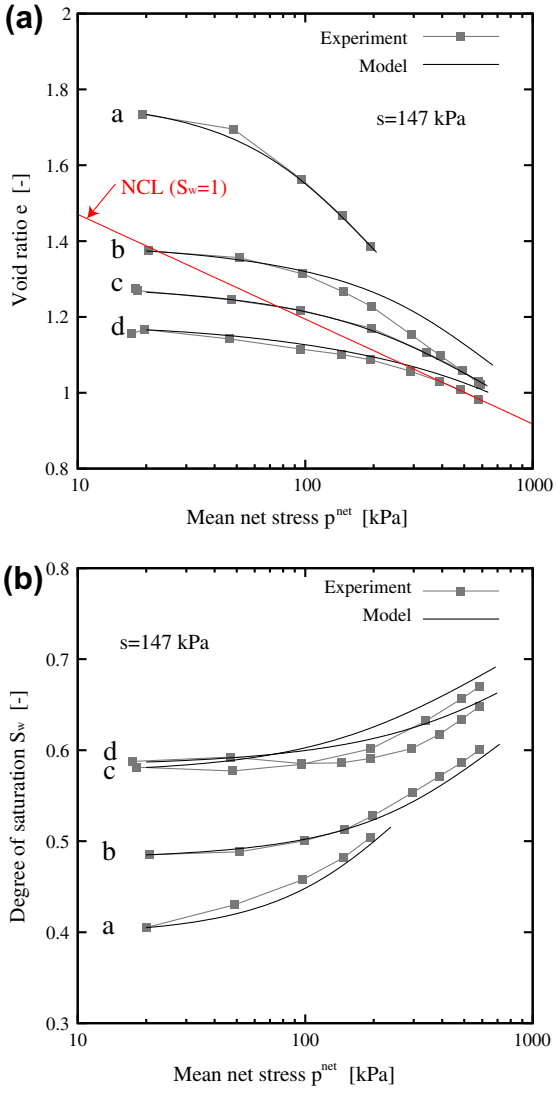

Fig. 6. Simulation of isotropic compression at constant suction. Data from [26].

5. Material constants

In this section we describe briefly the material constants for the hydraulic and mechanical model and give a short guide for their determination. The parameters of the hydraulic model correspond to the ones developed in Section 3. In total the hydraulic model requires nine parameters if all the one describing the main branches (including the residual degree of saturation) differs from their counterparts in the other main branch. On the other hand, the mechanical model requires seven parameters. An optimal calibration of the hydraulic model is achieved if the intrinsic water retention curves IWRC are available. If they are not, some approximations can be done using the water retention curves of samples with different initial densities. Therefore, a (modified) pressure plate test would be enough to calibrate the hydraulic component. For the mechanical model, the parameters can be calibrated using isotropic tests with controlled suction. An additional isotropic test with a saturated sample is also needed.

The main branches are described by the extended van Genuchten equation which presents the set of parameters $S^d_{w0}, S^i_{w0}, \alpha^d, \alpha^i, n^d, n^i$ and m_e. The parameters S^d_{w0}, S^i_{w0}, n^d and n^i are obtained by fitting these curves, the first pair at long values of suction $s \to \infty$ and the second pair trying to match the curvature of the IWRC. If these curves are not available, the pairs n^d and n^i can be adjusted on water retention curves obtained with overconsolidated samples, whereby lower variations of the void ratio e during the test are expected. The parameters α^d,α^i are adjusted fitting the dependence of the air entry suction with the suction and a value for m_e must be chosen such that it shifts properly the curves to the right for denser states. We have experienced that a value of $m_e \approx 1.3$ is a good approximation for many soils. The assumption $S^d_{w0} = S^i_{w0}$ and $n^d = n^i$ must not always hold, but is favorable to guarantee that the two main branches will not overlap each other.

The parameter κ_w must be calibrated at reversal points at the main branch at which $Y^{d/i} = 0$ (see Eq. (6)). At this point, if the volume changes is sufficient small $\dot{e} \approx 0$, the equation is reduced to $(\partial S_w/\partial s) = \kappa_w\left(\partial S^{s/d}_w/\partial s\right)$, and therefore κ_w can be calculated by measuring the current slope $(\partial S_w/\partial s)$ with the one at the bounding branch $\left(\partial S^{s/d}_w/\partial s\right)$. The exponent n_w can be calibrated by adjusting by trial and error the stiffness in a scanning line.

With respect to the mechanical model, the calibration of λ^{sat} and κ are obtained from isotropic tests with saturated samples by measuring the stiffness at loading and unloadung respectively in the e vs. ln (p) space. The reference point fixed by the parameters e_{ref} and p_{ref} is obtained by extending the normal consolidation lines for paths with different suction values, and intercepting them in the NCL for $S_w = 1$. The parameter r_m can be calibrated with a dry

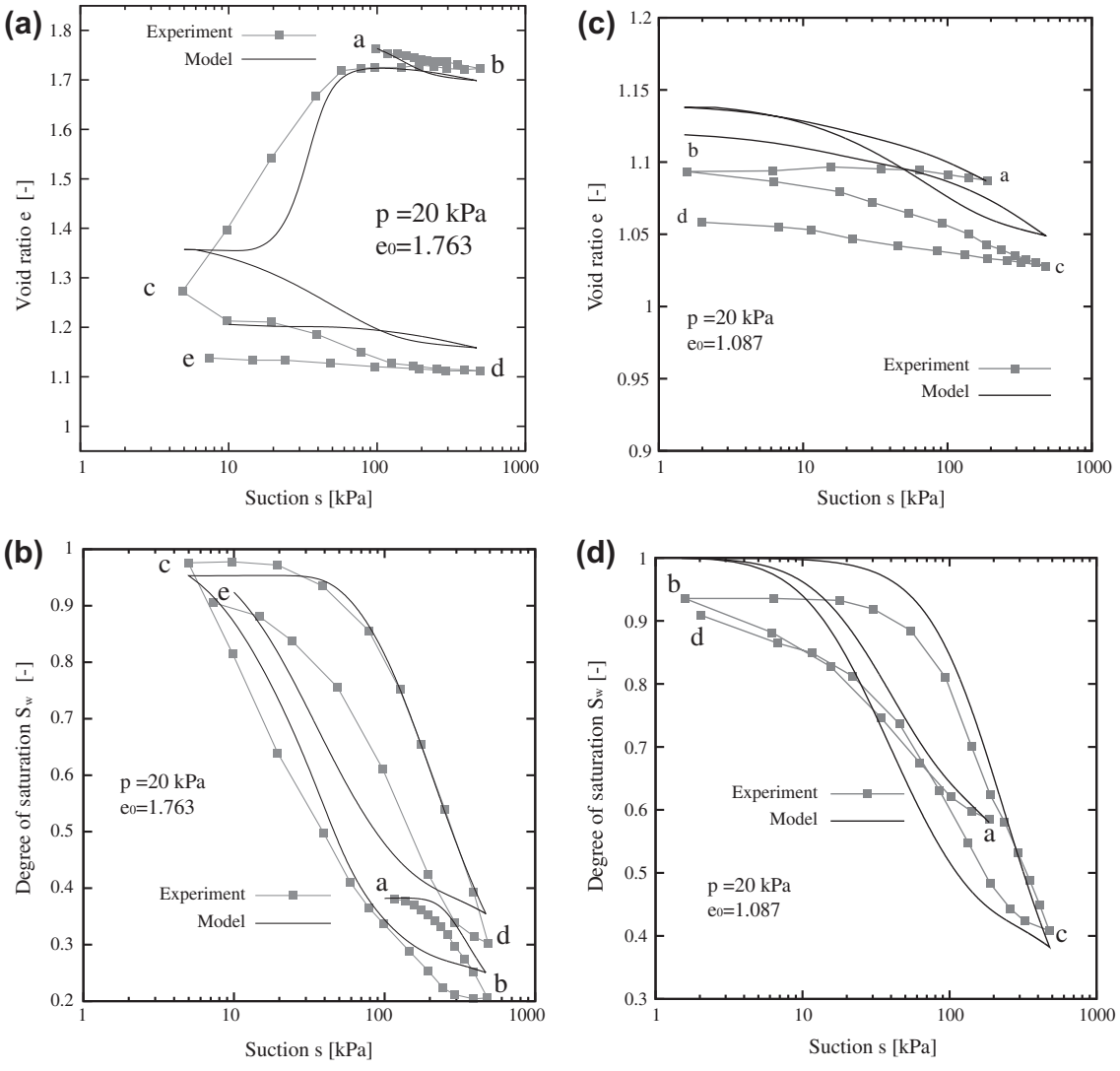

Fig. 7. Wetting–drying cycles under constant net stress p^{net} = const. Data from [26].

sample with $S_w = S^d_{w0}$. By solving Eq. (31) gives $r_m = (r-1)/\left(1 - S^d_{w0}\right)^{n_s} + 1$, where $r = \lambda/\lambda^{sat}$ can be calculated with the value of $\lambda = \lambda\left(S^d_{w0}\right)$ for this state. The exponent n_s can be approximated to $n_s = 3$ or fitted by trial and error to the curves. The parameter n_u should be calibrated with overconsolidated samples subjected to wetting $\dot{s} < 0$ upon constant net stress p^{net} = -const. Very high values of $n_u \to \infty$ allows volumetric contraction just for normal consolidated samples $p = p_i$. The units and recommended ranges for all these parameters are listed in Table 1.

Summary of equations.

Hydraulic model:
Given the functions $S_w = S^{d/i}(s,e)$ describing the main branches, the constitutive model is:

$$\dot{S}_w = \left(\kappa_w - (1-\kappa_w)Y^{d/i}\right)\frac{\partial S^{d/i}_w}{\partial s}\dot{s} - \frac{\partial S^{d/i}_w}{\partial e}(1+e)\dot{\varepsilon}_v$$

for $\dot{s} > 0$ then $Y^{d/i} = Y^d$ and $S^{d/i}_w = S^d_w$ and for $\dot{s} < 0$ then $Y^{d/i} = Y^i$ and $S^{d/i}_w = S^i_w$.
The interpolation functions Y^d and Y^i are:

$$Y^d = \left[\frac{\log(s/s^i)}{\log(s^d/s^i)}\right]^{n_w}, \quad \text{for } \dot{s} > 0$$

$$Y^i = \left[\frac{\log(s^d/s)}{\log(s^d/s^i)}\right]^{n_w}, \quad \text{for } \dot{s} < 0$$

where s^d and s^i are the projected suctions at the main drying and wetting curve respectively.
Mechanical model (just for isotropic states):
Constitutive equation:

$$\dot{p} = K(\dot{\varepsilon}_v - Y_i|\dot{\varepsilon}_v| + \sqrt{3}y\langle -\dot{s}\rangle), \text{ with } p = p^{net} + S_w s$$

Hypoelastic relations:

$$K = \frac{(1+e)p}{\lambda(1-Y_{im})}, \quad Y_{im} = \frac{r_{Km}-1}{r_{Km}+1} \text{ with } r_{Km} = \lambda/\kappa$$

Hypoplastic relations:

$$Y_i = \frac{r_K - 1}{r_K + 1}, \quad r_K = 1 + (r_{Km} - 1)\left(\frac{p}{p_i}\right)^{n_r}$$

Suction factor:

$$y = \frac{f_u A}{\sqrt{3}}\frac{(Y_i - 1)}{(1+e)}\frac{\partial e_i}{\partial S_w}$$

6. Application of the coupled models in element tests

The capabilities of the model are evaluated by simulating the experimental tests presented by Sun et al. [26,60] which clearly show the coupled hydro-mechanical behavior of the material. The set of experiments includes isotropic tests at constant suction, drying-wetting cycles and isotropic test at constant suction followed by wetting. The parameters were found according to the short guide given in Section 5 and are listed in the last column of Table 1. We have chosen a simple explicit algorithm for the hydraulic and mechanical model, each of them with a substepping scheme. No control of the substep size was performed but a small size was selected to assure the numerical convergence (maximum substep size were $\Delta\varepsilon_v = 10^{-4}$, $\Delta s = 1$ kPa).

The models were written in Fortran under the syntax of Umat for the program Abaqus using the entries for temperature as suction. The numerical integration was performed with Incremental Driver, developed originally by Niemunis [61] and extended by the authors of the present work to encompass its capabilities for the integration of coupled hydro-mechanical models.[5]

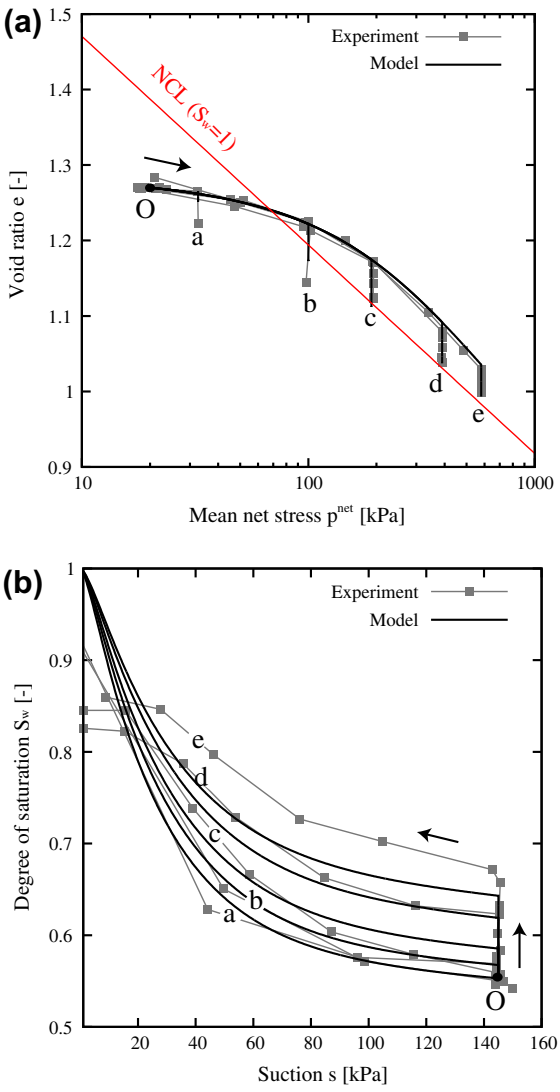

Fig. 8. Simulation of isotropic compression followed by wetting. Data from [26].

Fig. 6 shows four samples subjected to isotropic compression at the same suction s = 147 kPa but different initial void ratios e_0. The experiments show that while the sample densifies, the degree of saturation rises. This behavior is satisfactorily captured due to the coupling of the hydraulic model with the void ratio, which parallel affects the current value of the compression index λ.

The Fig. 7 shows the wetting–drying cycles of a loose sample (Fig. 7a and b) and a dense sample Fig. 7c and d. The specimens were isotropically compressed and then drying–wetting cycles were performed at constant mean net stress p^{net} = 20 kPa. The simulations show that under constant mean net stress p^{net} = const, the sample experiences volume contraction during the cycles (Fig. 7a and c) and a displacement of the SWCC (Fig. 7b and d) towards the right. The tests also show that after wetting some inclusted air remains for suction values lower than the water entry suction. The model was able to capture the volume contraction in the loose sample and the shift of the SWCC, however it assumes that $S_w = 1$ for $s = 0$ and therefore some discrepancies in the SWCC are appreciated after the wetting process.

[5] The new version of Incremental Driver can be free downloaded from http://www.rz.uni-karlsruhe.de/gn116/.

Fig. 8 shows five samples with the same initial conditions (at $t = 0$, $e = 1.27$, $S_w = 0.55$ and $s = 145$ kPa) which were isotropically compressed at constant suction $s = \text{const}$ till a certain value of mean net stress p^{net}. This final value of p^{net} varies for each sample. Subsequently, the samples were wetted $\dot{s} < 0$ and experienced a volumetric contraction. The simulations captured this behavior but once more the remaining degree of saturation after the process of wetting was not captured.

7. Final remarks

The article presented two coupled hydraulic and mechanical models for the simulation of unsaturated soils at isotropic states. The models were developed under the framework of hypoplasticity and have shown that this formulation is able to simulate the observed experimental behavior without the introduction of yield surfaces and plastic variables as in other models. Some parameters are shared with other existent constitutive models making easy its understanding. Of course, there are some limitations which were observed. For example, the model is not capable to reproduce the remaining degree of saturation S_w after a wetting process ending at $s = 0$ (not always $S_w = 1$ holds). In addition, the formulation of the mechanical model was limited for the isotropic states and therefore an extension for the three dimensional case is needed. Currently, the improvement of the aforementioned limitations are being studied and a new compression law which does not overlap the normal consolidation lines is in development.

Acknowledgments

The authors express their acknowledgements to the financial support provided by the DFG (German Research Council) corresponding to the research group FOR 1136.

Appendix A. Constraint for undrained material with residual water

Given a representative volume, the gravimetric water content w and degree of saturation S_w are defined as:

$$w = \frac{M_w}{M_s} \quad S_w = \frac{V_w}{V_v} \tag{A.1}$$

where M_i represents the mass of the phase $i = \{w, s, a, v\}$ (w = water, s = solid, a = air, $v = w + a$ are the voids) and V_i represents the volume of the phase i. Let us assume the water phase is decomposed into an active component and residual component such that $M_w = M_{wa} + M_{w0}$ and $V_v = V_{wa} + V_{w0}$ (the subindex $w0$ correspond to the residual component). The residual water phase corresponds to the water attached at the particles which does not disappear after a long process of drying. The active gravimetric content w_A and active degree of saturation S_A are defined as:

$$w_A = \frac{M_w - M_{w0}}{M_s}; \quad S_A = \frac{V_w - V_{w0}}{V_v} = S_w - S_{w0} \tag{A.2}$$

where S_{w0} is the residual degree of saturation and we assume that its rate is equal to zero $\dot{S}_{w0} = 0$. Using the relations above and defining the void ratio as $e = V_v/V_s$, one can show that the following relation holds between w_A and S_A assuming incompressible constituents:

$$S_A e = G_s w_A \tag{A.3}$$

where $G_s = (M_s V_w)/(M_w V_s)$ is the specific gravity considered by many authors a constant for a soil. The undrained condition is defined as $\dot{w} = 0$. Taking into account that M_{w0} is a constant by definition, when $\dot{w} = 0$ implies $\dot{w}_A = 0$. Therefore the undrained condition can be written as:

$$\begin{aligned} &\dot{S}_A e + S_A \dot{e} = 0 \quad \text{or,} \\ &\dot{S}_A = -\frac{S_A}{e}\dot{e} \end{aligned} \tag{A.4}$$

On the other hand, the hydraulic model is given by the following general equation:

$$\dot{S}_w = \dot{S}_A = \frac{\partial \dot{S}_w}{\partial \dot{s}}\dot{s} + \frac{\partial \dot{S}_w}{\partial \dot{e}}\dot{e} \tag{A.5}$$

Replacing Eq. (A.4) in (A.5) yields to the following relation:

$$-\left(\frac{S_A}{e} + \frac{\partial \dot{S}_w}{\partial \dot{e}}\right)\dot{e} = \frac{\partial \dot{S}_w}{\partial \dot{s}}\dot{s} \tag{A.6}$$

Sheng and Zhou [45] postulate that wetting paths $\dot{s} < 0$ under undrained and isotropic conditions experience always volumetric contraction $\dot{e} < 0$. Considering that the derivative $(\partial S_w/\partial s)$ is always negative, the following constraint from Eq. (A.6) is revealed:

$$\frac{\partial \dot{S}_w}{\partial \dot{e}} \geqslant -\frac{S_A}{e} = -\frac{S_w - S_{w0}}{e} \tag{A.7}$$

which recovers the constraint from Sheng and Zhou [45] when $S_{w0} = 0$.

Appendix B. Rewriting the hydraulic equation as hypoplastic equation

Eq. (5) can be written as a set of two equations for the case of drying $\dot{s} > 0$ and wetting $\dot{s} < 0$:

$$\begin{aligned} &\dot{S}_w = A_D \dot{s} \text{ for } \quad \dot{s} > 0 \\ &\dot{S}_w = A_I \dot{s} \text{ for } \quad \dot{s} < 0 \end{aligned} \tag{B.1}$$

where $A_D = \partial S_w^d/\partial s(\kappa_w - (1 - \kappa_w)Y^d)$ and $A_I = \partial S_w^i/\partial s(\kappa_w - (1 - \kappa_w)Y^i)$. The following relation is equivalent to the previous set of equations:

$$\dot{S}_w = \frac{1}{2}(A_D + A_I)\dot{s} + \frac{1}{2}(A_D - A_I)|\dot{s}| \tag{B.2}$$

which recalls the classical mathematical structure of hypoplastic models as in [30] when setting $L_s = (A_D + A_I)/2$ and $N_s = (A_D - A_I)/2$:

$$\dot{S}_w = L_s \dot{s} + N_s |\dot{s}| \tag{B.3}$$

References

[1] Prevost J. Mechanics of continuous porous media. Int J Eng Sci 1980;18:787–800.
[2] Ehlers W. On thermodynamics of elasto-plastic porous media. Arch Mech 1989;41:73–93.
[3] Boer R. The theory of porous media: highlights in historical development and current state. 1st ed. Berlin: Springer; 2000.
[4] Arduino A, Macari J. Implementation of porous media formulation for geomaterials. J Eng Mech 2001;127:157–66.
[5] Borja R. On the mechanical energy and effective stress in saturated and unsaturated porous materials. Int J Solids Struct 2006;43:1764–86.
[6] Gens A, Sanchez M, Sheng D. On constitutive modelling of unsaturated soils. Acta Geotech 2006;1:137–47.
[7] Houlsby G. The work input to an unsaturated granular material. Géotechnique 1997;47:193–6.
[8] Vaunat J, Romero E, Jommi C. An elastoplastic hydromechanical model for unsaturated soils. In: Experimental evidence and theoretical approaches in unsaturated soils. Trento, Italy; 2000. p. 121–38 [Balkema].
[9] Wheeler S, Sharma R, Buisson S. Coupling of hydraulic hysteresis and stress–strain behaviour in unsaturated soils. Géotechnique 2003;53(1):41–54.
[10] Nuth M, Laloui L. Effective stress concept in unsaturated soils: clarification and validation of a unified framework. Int J Numer Anal Meth Geomech 2008;32:771–801.
[11] Gens A. Soil environment interactions in geotechnical engineering. Géotechnique 2010;60:3–74.

[12] D'Onza F, Gallipoli D, Wheeler S, Casini F, Vaunat J, Khalili N, et al. Benchmark of constitutive models for unsaturated soils. Géotechnique 2011;61:283–302.
[13] Alonso E, Gens A, Josa A. A constitutive model for partially saturated soils. Géotechnique 1990;40(3):405–30.
[14] Sheng D. Review of fundamental principles in modelling unsaturated soil behaviour. Comput Geotech 2011;38:757–76.
[15] Guimaraes L, Sanchez M, Gens A, Sheng D. Developments in modelling the generalised behaviour of unsaturated soils. In: 1st European conference, E-UNSAT 2008. Durham, UK; 2008. p. 53–61.
[16] Josa A, Balmaceda A, Gens A, Alonso E. An elastoplastic model for partially saturated soil exhibiting a maximum collapse. In: 3rd International conference on computational plasticity, vol. 1. Barcelona; 1992. p. 815–26.
[17] Wheeler S, Sivakumar V. An elasto-plastic critical state framework for unsaturated soils. Géotechnique 1995;45:35–53.
[18] Cui Y, Delage P, Sultan N. An elasto-plastic model for compacted soils. In: Unsaturated soils, vol. 2; 1995. p. 703–9.
[19] Bolzon G, Schrefler B, Zienkiewicz O. Elastoplastic soil constitutive laws generalised to partially saturated states. Géotechnique 1996;46:279–89.
[20] Jommi C. Remarks on the constitutive modelling of unsaturated soils. In: International workshop on unsaturated soils. Trento; 2000. p. 139–53.
[21] Gallipoli D, Gens A, Sharma R, Vaunat J. An elastoplastic model for unsaturated soil incorporating the effects of suction and degree of saturation on mechanical behaviour. Géotechnique 2003;53:123–35.
[22] Sheng D, Sloand S, Gens A. A constitutive model for unsaturated soils: thermomechanical and computation aspects. Comput Mech 2004;33: 453–65.
[23] Tamagnini R. An extended cam-clay model for unsaturated soils with hydraulic hysteresis. Géotechnique 2004;54:223–8.
[24] Borja R. Cam-clay plasticity. part v: a mathematical framework for three-phase deformation and strain localization analyses of partially saturated porous media. Comput Meth Appl Mech Eng 2004;193:5301–38.
[25] Sheng D, Gens A, Fredlund D, Sloan S. Unsaturated soils: from constitutive modelling to numerical algorithms. Comput Geotech 2008;35:810–24.
[26] Sun D, Sheng D, Cui H, Sloan W. A density-dependent elastoplastic hydro-mechanical model for unsaturated compacted soil. Int J Numer Anal Meth Geomech 2007;31:1257–79.
[27] Zhou A, Sheng D, Sloan S, Gens A. Interpretation of unsaturated soil behaviour in the stress-saturation space, i: volume change and water retention curve. Comput Geotech 2012;43:178–87.
[28] Gonzalez N, Gens A. Evaluation of a constitutive model for unsaturated soils: stress variable and numerical implementation. In: E A, A G, editors. Unsaturated soils, vol. 2. CRC Press; 2011. p. 829–36.
[29] Solowski W, Galipolli D. Explicit stress integration with error control for the barcelona basic model. part 1: algorithms formulation. Comput Geotech 2009;37:59–67.
[30] Wolffersdorff V. A hypoplastic relation for granular materials with a predefined limit state surface. Mech Cohes-Frict Mater 1996;1:251–71.
[31] Masin D. A hypoplastic constitutive model for clays. Int J Numer Anal Meth Geomech 2005;29(4):311–36.
[32] Niemunis A, Grandas C, Prada L. Anisotropic visco-hypoplasticity. Acta Geotech 2009;4:293–314.
[33] Fuentes W, Triantafyllidis T, Lizcano A. Hypoplastic model for sands with loading surface. Acta Geotech 2012;7:177–92.
[34] Gudehus G. A comprehensive concept for non-saturated granular bodies. In: 1st International conference on unsaturated soils, vol. 2. Paris; 1995. p. 725–27.
[35] Bauer E, Tantono S, Cen W, Zhu Y, Kast K. Hypoplastic modeling of the disintegration of dry and saturated weathered broken rock. In: Schanz T, editor. Theoretical and numerical unsaturated soil mechanics Springer proceedings in physics, vol. 113. Berlin Heidelberg: Springer; 2007. p. 11–8.
[36] Niemunis A. Extended hypoplastic models for soils. Habilitation, Schriftenreihe des Institutes fnr Grundbau und Bodenmechanil der Ruhr-UniversitSt Bochum, Germany, heft 34; 2003.
[37] Masin D, Khalili N. A hypoplastic model for mechanical response of unsaturated soil. Int J Numer Anal Meth Geomech 2008;32:1903–26.
[38] Khalili N, Khabbaz M. A unique relationship for χ for the determination of the shear strength of unsaturated soils. Géotechnique 1998;48:1–7.
[39] Khalili N, Zargarbashi S. Influence of hydraulic hysteresis on effective stress in unsaturated soils. Géotechnique 2010;60:729–34.
[40] Gardner W. Some steady-state solutions of the unsaturated moisture flow equation with applications to evaporation from water table. Soil Sci 1958;85:228–32.
[41] Brooks R, Corey A. Hydraulic properties of porous medium. Hydrology papers Colorado State University, vol. 3; 1964. p. 24.
[42] van Genuchten M. A closed-form equation for predicting the hydraulic conductivity of unsaturated soils. Soil Sci Soc Am J 1980;44:892–8.
[43] Fredlund D, Xing A. Equations for the soil–water characteristic curve. Can Geotech J 1994;31:521–32.
[44] Morvan M, Wong H, Branque D. Incorporating porosity-dependent hysteretic water retention behavior into a new constitutive model of unsaturated soils. Can Geotech J 2011;48:1855–69.
[45] Sheng D, Zhou A. Coupling hydraulic with mechanical models for unsaturated soils. Can Geotech J 2011;48:826–40.
[46] Li X. Modelling of hysteresis response for arbitrary wetting/drying paths. Comput Geotech 2005;32:133–7.
[47] Liu C, Muraleetharan K. Description of soil water characteristic curves using bounding surface plasticity theory. In: Fourth international conference on unsaturated soils, vol. 2; 2006. p. 2432–40.
[48] Wei C, M D. Formulation of capillary hysteresis with internal state variables. Water Resour Res 42;1996:1–16.
[49] Liu C, Muraleetharan K. Coupled hydro-mechanical elastoplastic constitutive model for unsaturated sands and silts. i: formulation. Int . Geomech ASCE 2012;12:239–47.
[50] Romero E. Characterisation and thermo-mechanical behaviour of unsaturated. Boom clay: an experimental study. Ph.D. thesis, UPC, Barcelona; 1999.
[51] Vanapalli S, Fredlund D, Pufahl D. The influence of the soil structure and stress history on soil–water characteristics of a compacted till. Géotechnique 1999;49:143–59.
[52] Gallipoli D, Wheeler S, Karstunen M. Modelling the variation of degree of saturation in a deformable unsaturated soil. Géotechnique 2003;53(2):105–12.
[53] Lee I, Sung S, Cho G. Effect of stress state on the unsaturated shear strength of a weathered granite. Can Geotech J 2005;42:624–31.
[54] Nuth M, Laloui L. Advances in modelling hysteretic water retention curve in deformable soils. Comput Geotech 2008;35(6):835–44 [special Issue on Unsaturated Soils: Models, Algorithms and Application].
[55] Masin D. Predicting the dependency of a degree of saturation on void ratio and suction using effective stress principle for unsaturated soils. Int J Numer Anal Meth Geomech 2010;34:73–90.
[56] Wei W, Kolymbas D. Numerical testing of the stability criterion for hypoplastic constitutive equations. Mech Mater 1990;9:245–53.
[57] Zhang F, Ikariya T. A new model for unsaturated soil using skeleton stress and degree of saturation as state variables. Soils Found 2011;51:67–81.
[58] Masin D, Herle I. State boundary surface of a hypoplastic model for clays. Comput Geotech 2005;32(6):400–10.
[59] Bauer E. Calibration of a comprehensive constitutive equation for granular materials. Soils Found 1996;36:13–26.
[60] Sun D, Sheng D, Sloan W. Elastoplastic modelling of hydraulic and stress–strain behaviour of unsaturated soils. Mech Mater 2006;39:212–21.
[61] Niemunis A. Incremental Driver, user's manual. University of Karlsruhe KIT, Germany, March 2008.